Korean J. Chem. Eng., 33(11), 3050-3068 (2016)
DOI: 10.1007/s11814-016-0236-x
pISSN: 0256-1115
eISSN: 1975-7220

REVIEW PAPER

A review on numerical consideration for computational fluid dynamics modeling of jet mixing tanks

Eakarach Bumrungthaichaichan†

Department of Chemical Engineering, Faculty of Engineering, King Mongkut's Institute of Technology Ladkrabang, Bangkok 10520, Thailand

(*Received 27 April 2016 • accepted 15 August 2016*)

Abstract−Over two decades or so, the computational fluid dynamics (CFD) modeling of various jet mixing tank configurations was developed and published. Further, the studies of various parameters used in experimental and CFD works were also reviewed to obtain the optimal design procedure. However, the numerical setup for jet mixing tank modeling was not studied and reported. Hence, in this review paper, the important numerical setup for CFD simulation of jet mixing tanks, including numerical solution techniques, turbulence model selection, boundary conditions, numerical methods, solution strategy, and CFD grid, are clearly demonstrated to achieve the comprehensive CFD modeling guideline for jet mixing tank. Further, the validations for jet mixing tank models are also represented.

Keywords: CFD, Jet, Mixing, Modeling, Numerical Method

INTRODUCTION

Mixing is one of the most important chemical process industries. There are two common ways to achieve liquid mixing in a tank, including impeller stirred tank and jet mixed tank. The mixing time of jet agitated tanks is shorter than the conventional stirred tanks [1]. Generally, for jet mixing tank, the liquid is drawn into a pump and discharges as a high velocity liquid jet through a nozzle into the slow-moving or stationary liquid. Then, the primary liquid jet entrains the surrounding liquid and creates liquid circulation inside the vessel. Thus, the different components inside the tank are mixed. The mixing inside the jet mixed tank is obtained by the following processes [2]: (i) Bulk transport of jet liquid from the jet nozzle to remote areas of the tank. (ii) Bulk transport, induced by jet flow in remote areas of the tank. (iii) Bulk transport, induced by entrainment of secondary liquid into the jet. (iv) Mixing of the jet and secondary liquids (may be the same liquid) within the jet flow.

The typical jet mixing tank geometries are shown in Fig. 1. A batch jet mixing tank, which liquid B is directly added to the primary liquid A contained in a tank and the tank in which liquid B is added to the recycle line are illustrated in Fig. 1(a) and Fig. 1(b), respectively. Further, the continuous jet mixing tank, which liquids A and B are directly fed into the tank, is shown in Fig. 1(c).

The jet mixing tanks are widely used in many processes because jet mixed tanks are cheaper and easier to install, and do not require the additional support for their structures. Further, the jet mixing tanks are also easier for maintenance because of the absence of moving parts. There are many applications of jet mixing tanks, such as blending the inhibitor to stop runaway reactions [3,4], emergency

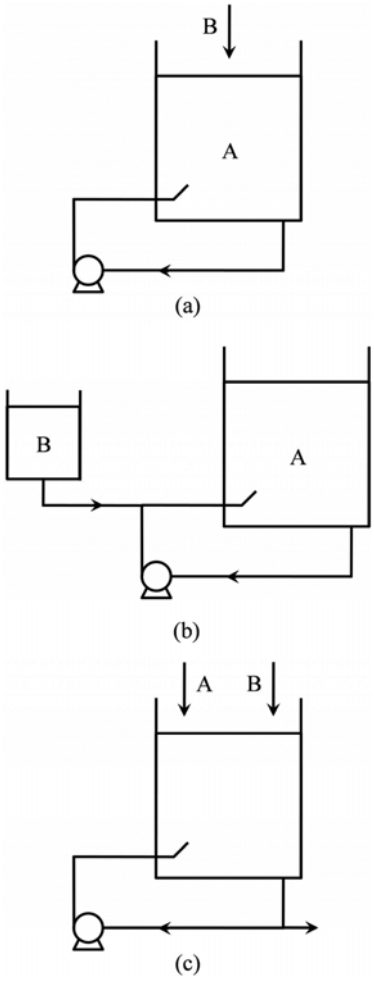

Fig. 1. Schematics of (a) batch jet mixing tank (direct addition of liquid B) (b) batch jet mixing tank (addition of liquid B into recycle line) (c) continuous jet mixing tank [2].

†To whom correspondence should be addressed.
E-mail: b_eakarach@hotmail.com

cooling systems [5], homogenization in hydrocarbon and LNG storage tanks [6,7], jet reactors in various processes [8,9], and mixing of acid [10].

There have been many extensive experimental studies of jet mixing tank for over 60 years. One of the earliest such studies was by Fossett and Prosser [6], who first introduced the idea of liquid jet mixer. They used the inclined side entry jet mixing tanks with jet Reynolds number (Re_j) of 4,500-80,000 to investigate the mixing time correlation. Fossett [1] modified the previous mixing time correlation of Fossett and Prosser [6] and showed that the jet mixing tanks exhibited a shorter mixing time as compared to the conventional mixing tanks. Fox and Gex [11] investigated the mixing times in tanks with the different ratios of liquid height (H) to tank diameter (D), and found that the mixing time was dependent on the momentum flux added to the tank.

Furthermore, van de Vusse [12] used inclined side entry jet mixing tanks and reanalyzed the data obtained by Fox and Gex [11] to investigate the mixing time correlation. Okita and Oyama [13] proposed a more reliable mixing time correlation by adding the liquid height into the correlation. Coldrey [14] showed the modified design of inclined side entry jet mixing tank. Furthermore, the jet path length was taken into account the jet mixing time. Hiby and Modigell [15] studied the axial jet in cylindrical tank with flat base and showed that the mixing time was dependent on jet Reynolds number when the jet Reynolds number was less than 1,000,000. Lehrer [16] studied the mixing of miscible fluids with different densities for axial jet mixing and developed the mixing time model. Moreover, he compared his model with the results reported by Fox and Gex [11].

Lane and Rice [17] studied a vertical jet mixing tank with a hemispherical base and revealed that the mixing time strongly depended on jet Reynolds number in the laminar regime, but slightly depended on turbulent jet Reynolds number. Lane and Rice [18] extended their work and proposed that the tank with longest jet path length

Table 1. Previous jet mixing time correlations

Authors	Geometry	Dimension	Correlation
Fossett and Prosser (1949)	Cylindrical tank with inclined side entry jet	D=1.524 m H=0.9144 m d_j=1.9 mm d_o=2.54 cm θ=40° Re_j=4,500-80,000	$t_m = 9\frac{D^2}{U_j d_j}$
Fossett (1951)	Cylindrical tank with inclined side entry jet	D=1.524 m H=0.9144 m d_j=1.9 mm d_o=2.54 cm θ=40°	$t_m = C_P\frac{D^2}{U_j d_j}$ C_P=9 when $t_{inj}>t_m/2$ C_P=4.5 when $t_{inj}<t_m/2$
Fox and Gex (1956)	Cylindrical tank with side entry jet	D=0.15-4.27 m H=0.15-4.27 m d_j=0.159-3.81 cm U_j=0.6-11 m/s	$t_m = f\frac{H^{0.5}D}{(U_j d_j)^{4/6} g^{1/6}}$ $f = 95.638 Re_j^{-0.146}$
Van de Vusse (1959)	Cylindrical tank with inclined side entry jet	-	$t_m = 3.68\frac{D^2}{U_j d_j}$
Okita and Oyama (1963)	Cylindrical tank with inclined side entry jet	-	$t_m = 2.6\frac{D^{1.5}H^{0.5}}{U_j d_j}$
Coldrey (1978)	Cylindrical tank with inclined side entry jet	-	$t_m = 4.507\frac{D^2 H}{L U_j d_j}$
Hiby and Modigell (1978)	Cylindrical tank with axial jet	-	$t_m = T^*\frac{D^2}{U_j d_j}$ T^*=2.3 when Re_t>1,000,000 $T^* \propto Re$ when Re_t<1,000,000
Lehrer (1981)	Axial jet	Free turbulent jet	$t_m = \frac{0.658}{U_j}\left(\frac{\rho_c}{\rho_d}\right)^{5/8} d_j^{0.25} \times \left(\frac{U_j}{N_j A}\right)^{3/4} [-\log(1-c^*)]$
Lane and Rice (1981)	Cylindrical tank with axial jet	For axial jet D=0.31-0.57 m H/D=0.5-3.0 Re_j=250-60,000	$t_m = C_1\frac{H^{0.5}D^{0.75}}{Re_j^{1.3}(U_j d_j)^{0.5} g^{0.25}}$ Re_j<1,800 $t_m = C_2\frac{H^{0.5}D^{0.75}}{Re_j^{0.15}(U_j d_j)^{0.5} g^{0.25}}$ Re_j>1,800

Table 1. Continued

Authors	Geometry	Dimension	Correlation
Lane and Rice (1982)	Cylindrical tank with side entry jet and axial jet	For side entry jets D=0.31-0.57 m H/D=0.9-1.1	$t_m = f\frac{H^{0.5}D}{(U_j d_j)^{0.667} g^{0.166}}$ $f = 113.133 Re_j^{-0.146}$
		For axial jets D=0.31-0.57 m H/D=0.5-3.0 Re_j=250-60,000	
Maruyama et al. (1982)	Cylindrical tank with inclined side entry jet	D=56, 104 cm H=84, 125 cm h_i, h_o=4.38, 20.5, 48.5 cm, (D=56 cm) h_i, h_o=4, 14, 24, 44, 74, 94 cm (D=104 cm) d_j=0.5, 1, 1.8 cm θ=7°, 15°, 30°, 45°, 54°, 60°, 73°	$\left(\frac{t_m}{t_r}\right)\left(\frac{L}{d_j}\right) = 2.5 - 8.0$ Re_j>30,000
Simon and Fonade (1993)	Two jets at H/2 and H/3, horizontally located	D, H=490 mm d_j=10 mm	$M = t_m (gH)^{0.5} D J_s^{2/3} \approx 1$ $J_s = \frac{J}{\rho U_j g}$, $J = \rho A U_j^2$
Orfaniotis et al. (1996)	Two jets at H/2 and H/3, horizontally located	D, H=500 mm d_j=9, 15 mm	$M = \left(\frac{t_m}{t_r}\right) J_s^{0.41} = 11.3$ $t_r = \frac{D}{(gH)^{0.5}}$ $J_s = \frac{J}{\rho U_j g}$, $J = \rho A U_j^2$
Grenville and Tilton (1996)	Cylindrical tank	D=0.61-36 m H/D=0.2-1.0 d_j=5.8-50 mm U_j=2.2-24.8 m/s	$t_m = 3\frac{L^2}{U_j d_j}$
Grenville and Tilton (1997)	Cylindrical tank	Same as Grenville and Tilton (1996)	$k_m = k\frac{D^2 H}{U_j d_j L}$ k=9.34 when θ>15° k=13.8 when θ<15°
Grenville and Tilton (2011)	Cylindrical tank	D=0.61-36 m H/D=0.2-4.0	$\frac{U_j t_m}{d_j}\left(\frac{d_j}{L}\right)^2 = 2.95$

exhibited the minimum mixing time, which was similar to the previous suggestion of Coldrey [14]. Maruyama et al. [19] studied the jet mixing time and found that the mixing time depended on liquid depth, nozzle height, and nozzle angle. Maruyama [20] studied the jet mixing time for different jet injection angles and showed that the angles of 25-30° and 75° showed the local minimum blending time. Simon and Fonade [8] and Orfaniotis et al. [21] studied the jet mixing tanks and proposed the mixing time correlation for steady and unsteady jets.

Grenville and Tilton [22] reanalyzed the previous data of Grenville et al. [23] and showed the mixing time correlation, based on the turbulent kinetic energy dissipation rate at the jet path end. Grenville and Tilton [24] proposed a correlation based on jet nozzle angle and compared their model with the circulation time model and found that both models can be used to predict accurate mixing time in the tank with H/D less than unity. They also showed that the mixing time was significantly increasing when the injection angle was less than 15°. Grenville and Tilton [25] extended their work by studying the mixing time in various tank geometries (0.2<H/D<4) and found that their jet turbulence model fitted all data for 0.2<H/D<3.

Patwardhan and Gaikwad [26] studied the effects of various parameters, including nozzle diameter, jet nozzle angle, and jet velocity, on mixing time. They found that the mixing time of horizontal jet was larger as compared to the inclined jet. The tank with jet nozzle angle of 45° showed the minimum mixing time as compared to the other jet nozzle angles. The mixing time was found to decrease with increasing the nozzle diameter. These jet mixing tank geometries and their jet mixing time correlations are summarized in Table 1.

There are many studies on the experiments of jet mixing tanks; however, the only available information is the overall mixing time for the given parameters. Details of circulation and mixing pattern within the tanks are not available. The shortfalls of experiment in jet mixing tanks can be drawn as the following:

(i) The first limitation of the correlations presented in Table 1 is that there is no universal correlation for predicting the mixing time. They predict well only over the range of studied parameters, i.e., correlations are case specific.

(ii) Many correlations do not consider the liquid height, meaning that the mixing times are identical in all the tanks that have the same diameter, jet velocity and jet diameter regardless of the liquid height.

(iii) The jet path length is commonly defined as a distance between jet nozzle exit and the tank wall or liquid surface. This jet path length is only a geometric parameter, which is not an actual jet path length. However, in tall tanks the jet may lose its momentum before it impinges the opposite boundaries. In this case, the jet path length may be overestimated.

(iv) Effects of density and viscosity of liquid and presence of solid particles on mixing time are limited in a narrow range.

(v) The information of measuring probe, which is used to identify the mixing time, locations, is not reported. It is not clear if the mixing inside a tank is indicated by a single measuring probe. Furthermore, the measuring probes may be considered as the obstacles inside the tank. The flow pattern inside the vessels may be disturbed by these measuring probes.

In the last three decades or so, computational fluid dynamics (CFD) [27-29], which is based on the numerical solutions of partial differential equations, has become important because it produces large volumes of results with inexpensive operating cost. And it can provide clear insight into many fluid flow phenomena. Recently it has been employed in a broad range of applications, such as the prediction of a simple fluid flow in pipe [30,31], the prediction of fluid flow pattern and mixing inside the stirred tank [32,33], the prediction of complex fluid flow field and collection efficiency of cyclone separator [34,35], etc. For jet mixing tank, CFD is also employed to study the jet mixing tank and address the shortfalls of experiment in jet mixing tanks.

Brooker [36] investigated the jet mixer by using CFD technique. For validation of the model, only one nozzle geometry with a single probe location was used to achieve the overall mixing time. The results revealed that CFD predicted mixing time with maximum error of about 15%. Hoffman [4] showed the CFD simulation of jet mixing in a large storage tank. The simulations were carried out for only one half of the tank with 24,360 nodes. However, the model was not validated by comparing with the experimental data. Ranade [37] employed the CFD with standard k-epsilon turbulence model to simulate the alternating jet mixed tank. The results showed that the presence of alternating jet did not always lead to the reduction in mixing time.

Jayanti [38] studied the hydrodynamics inside the side entry and axial jet mixing tanks by CFD simulations. Good agreement between CFD simulations and experimental data was achieved. The results showed that the key factor in reducing mixing time was minimizing or eliminating dead zones in the reactor, e.g., the tank with a conical bottom. Patwardhan [39] developed a CFD model to predict the mixing behavior in jet mixed tanks. The predicted results were compared with the experimental measurements over a wide range of jet velocities, nozzle angles, and nozzle diameters. He showed that the CFD model predicted the overall mixing time well, but the predicted concentration profiles were not in good agreement with experiment. Moreover, he found that these incorrect concentration profiles can be improved by adjusting the turbulence model parameters.

Zughbi and Rakib [40] and Zughbi and Ahmad [41] employed different turbulence models to simulate the jet mixing tanks. They concluded that the standard k-epsilon was the optimal turbulence model because of its accuracy and time efficiency. Jaiklom et al. [42] showed CFD simulations of two different jet injections, including free jet and wall jet. Good agreement in concentration profiles was achieved between the numerical results and experimental data. The results revealed that the free jet injection showed better mixing as compared to the wall jet injection.

The studies of various parameters used in experimental and CFD works were reviewed by Wasewar [43] to achieve the optimal design procedure. Since this review was published, the CFD modeling for jet mixing tanks has been developed and published. An updated review is necessary to obtain a comprehensive CFD modeling for jet mixing tank. Thus, in this review paper, the numerical setup for jet mixing tank CFD simulations are clearly demonstrated, including numerical solution techniques, turbulence model selection, boundary conditions, numerical methods, solution strategy, and CFD grid. Model validations for jet mixing tanks are also represented.

JETS AND JET MIXING TANKS

1. Fluid Dynamics of Jets

Jet is one of the most important free shear flows, for which there is no direct wall effect on the flow. It can be observed in various applications, such as jet reactor, combustion chamber, and jet mixing tank. Generally, the turbulent jet discharges through a circular nozzle into the stationary fluid or slow-moving fluid, which is known as turbulent round jet. A jet is considered as a fully turbulent jet at a jet Reynolds number (Re_j) above about 1000-2000 and laminar jet for Re_j below about 100 [2]. There are three distinguished layers of the jet flow, including centerline layer, shear layer region, and outer region layer [44], as shown in Fig. 2. In jet shear layers, the mixing process involves bulk mixing driven by large-

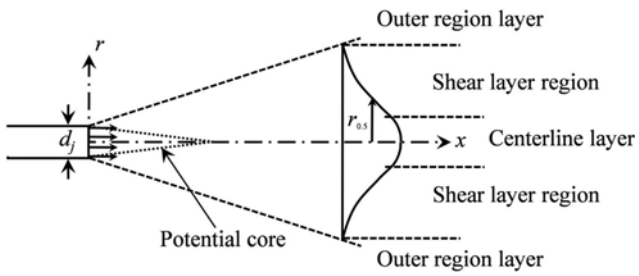

Fig. 2. Details of round jet layers [44].

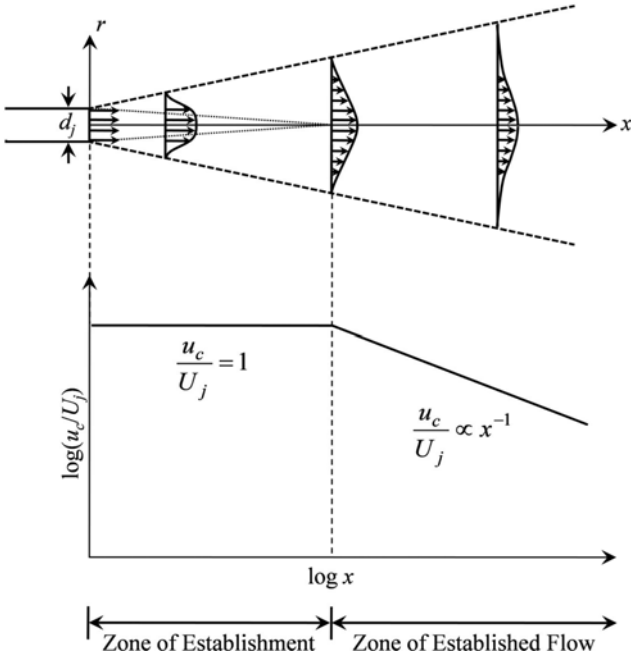

Fig. 3. Schematic of axis-symmetric turbulent round jet.

scale coherent structures (CS) and smaller-scale mixing dominated by turbulent velocity fluctuations [45]. The schematic of axis-symmetric turbulent round jet discharges from a nozzle with an exit velocity U_j is shown in Fig. 3.

From Fig. 3, there are two different regions in turbulent jets [46]. In the first region, the mean centerline velocity (u_c) is equal to discharge velocity (U_j) and the turbulent mixing has not penetrated into the jet center. This zone is known as the potential core region. The region between the jet nozzle exit and the end of potential core is called the zone of flow establishment (ZFE). The second region is the region beyond the potential core zone, which is known as the zone of established flow (ZEF). In ZEF, the mixing penetrates into jet centerline and the mean centerline velocity is found to decrease with increasing longitudinal distance (x). The transverse velocity profiles show Gaussian distribution.

The jet centerline velocity (u_c) of turbulent jet can be evaluated by the correlation of Davies [47] as shown in Eq. (1).

$$u_c=6.4\frac{d_jU_j}{x},\ \text{for}\ \frac{x}{d_j}>6.4 \tag{1}$$

For radial distribution, Schlichting [48] represented the radial profile of the jet axial velocity (u) as:

$$u=\frac{3}{8\pi}\frac{K}{\nu_0 x}\frac{1}{\left[1+\frac{1}{4}\eta^2\right]^2} \tag{2}$$

where $\eta=\frac{1}{4}\sqrt{\frac{3}{\pi}}\frac{K^{1/2}}{\nu_0}\frac{r}{x}$, $K^{1/2}=1.59b_{1/2}u_c$, $\nu_0=0.0256b_{1/2}u_c$, $b_{1/2}=0.0848x$, $u_c=7.31\frac{d_jU_j}{x}$

Another equation for the radial distribution of the jet axial velocity was reported by Davies [47] as:

$$\log_{10}\left[\frac{u_c}{u}\right]=40\left[\frac{r}{x}\right]^2,\ \text{for}\ 7<\frac{x}{d_j}<100 \tag{3}$$

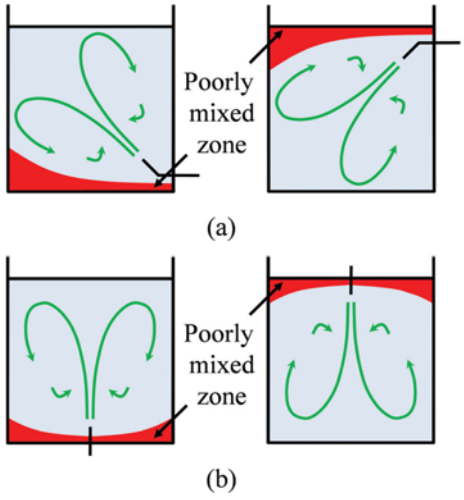

Fig. 4. Schematics of (a) side entry jet mixing tanks (b) axial jet mixing tanks.

In jet flow, the interest phenomenon is entrainment. Albertson et al. [49] revealed that, for round free jet, the entrainments of two different regions are not identical. For ZFE, the equation for jet entrainment can be written as:

$$\frac{Q}{Q_0}=1+0.083\frac{x}{d_j}+0.0128\left[\frac{x}{d_j}\right]^2,\ \text{for}\ \frac{x}{d_j}\le 6.2 \tag{4}$$

The equation of jet entrainment in ZEF is given by

$$\frac{Q}{Q_0}=0.32\frac{x}{d_j},\ \text{for}\ \frac{x}{d_j}>6.2 \tag{5}$$

where Q and Q_0 are jet entrainment and jet efflux rates, respectively.

2. Fluid Dynamics of Jet Mixing Tanks

There are two common types of jet mixed tank, including side entry jet and axial jet. The flow pattern generated by these two different tanks is shown in Fig. 4. The overall flow can be described as [2]:

(i) Lateral expansion of the jet due to entrainment as the jet penetrates the secondary liquid. The velocity and turbulence of the jet flow decrease because the jet flow momentum is spread over a steadily increasing flow area.

(ii) Rollover of the jet flow when it hits the tank wall or base or liquid surface.

(iii) After rollover, a very weak liquid motion driven by the jet flow along the tank wall or base or liquid surface.

(iv) Liquid flow induced by jet entrainment from remote regions towards the jet.

The degree of mixing is limited by the poor mixing regions depicted in Fig. 4, meaning that the poor mixing zones are the last regions where the given degree of mixing is achieved. The size of poorly mixed region (mixing time) is affected by jet nozzle position, recycle suction position, tank and jet sizes, jet protrusion, liq-

uid height, and tank base shape. The main objective of jet mixing design is to minimize these poor mixing regions by producing the liquid motion in a whole tank.

3. Mixing Time Investigation

Mixing time is an important parameter in mixing devices. It can be investigated by two different techniques: tracer technique and visual observation technique. These techniques measure the macro-mixing inside the tanks, i.e., they can be used to indicate the time taken to achieve a given degree of homogeneity throughout the whole vessel.

For tracer technique, generally, a tracer (electrolyte solution) is injected into the tank. The time history of tracer concentration is then measured at a single specific point or at the several specific points inside the tank. The mixing time (t_m) is defined as the time at which the concentration (c) has reached (or nearly reached) the final mean tracer concentration ($\bar{c}$). If there is no tracer inside the tank, then a mixing time can be measured as the time from tracer addition to the time when

$$\frac{|c-\bar{c}|}{\bar{c}} = m \tag{6}$$

where m is the maximum acceptable absolute value of the relative deviation of the mix [50]. When complete homogeneity (mixing) is achieved, m is equal to 0. In an experiment, there are two general criteria to quantify the mixing. Some experimental works used 99% mixing to indicate the mixing time [18,22,23,51]. However, 95% mixing is also commonly used as a mixing criterion [2,39, 40,52]. Hence, m is equal to 0.01 for 99% mixing or 0.05 for 95% mixing.

Temperature can also be measured to obtain the mixing time [14,40]. The 95% mixing is obtained when the temperature anywhere inside the tank is within the range of $\overline{T}\pm(\overline{T}-T)\times0.05$, where $\overline{T}$ and T, respectively, are the final mean value of temperature and the initial temperature of the bulk liquid in the mixing tank [40].

For visual observation, the liquid is first made weakly acidic and an indicator is added. A sufficient quantity of strong base is then added to neutralize the acid. The mixing time is measured as the time from the moment of base addition to the time at which color of the indicator disappears.

In CFD simulation, the tracer technique is commonly used to determine the mixing time. For tracer concentration technique, the tracer may be patched inside the tank domain [37,39,53] or injected into the tank [38,54,55] to introduce the tracer for unsteady state simulation. Then, the time-history of the tracer concentration for the various specified probes is recorded and used to identify the mixing time. The measured variable can be temperature. In temperature technique, a known volume of fluid with a desired temperature is specified inside the domain. The time-history of temperature is then monitored and employed to investigate the mixing time. This technique was successfully used in many CFD simulations [40,41].

CFD MODELING OF JET MIXING TANKS

Computational fluid dynamics (CFD) uses numerical methods and algorithms to solve and analyze fluid flow phenomena, heat transfer, and chemical reaction. As mentioned, the CFD technique was successfully adopted to simulate the jet mixing tank. In this section, the numerical methods are reviewed and summarized to achieve the comprehensive CFD modeling guideline for jet mixing tank.

1. Numerical Solution Techniques

In fluid dynamics, the fluid flow governing equations are partial differential equations (PDEs). The analytical solutions for most fluid flow problems may not be obtained because of the nonlinearity in PDEs. However, this problem can be resolved by using numerical method. The numerical solutions can be achieved by hand or computer calculations. Nowadays, the computer performance is successfully developed, which makes it possible to do the fluid flow experiments on the computer alone. The idea of computer experiments was first published by Harlow and Fromm [56]. Here, the computational fluid dynamics (CFD) is born.

There are three general numerical solution techniques--finite difference method (FDM), finite element method (FEM), and finite volume method (FVM)--for fluid flow problems. Generally, numerical solver performs the following steps:

(i) Approximation of the unknown flow variables by means of simple functions.

(ii) Discretization by substitution of the approximations into the governing flow equations and subsequent mathematical manipulations.

(iii) Solution of the algebraic equations.

The main differences between these methods are associated with the way in which the flow variables are approximated and with the discretization processes [28].

The oldest technique is the finite difference method [57]. It successfully showed the first ever numerical solutions of low speed flow past the cylinder [58]. Over a century, various numerical techniques were developed to solve fluid flow phenomena.

One of the developed numerical techniques is the finite element method, which was originally developed for structural mechanics, and also developed to solve fluid flow problems in middle to late 1970s. In the past, the Galerkin finite element method (GFEM) was used as a numerical technique. It was successfully applied to the problems governed by self adjoint PDEs, e.g., structural mechanics, heat conduction, etc. However, the GFEM failed to predict fluid flow problems because the fluid flow governing equations (Navier-Stokes equations) are non-self adjoint PDEs. So, other finite element methods were developed to solve fluid flow problems [59,60].

Another numerical technique in fluid dynamics is the finite volume method, which is a special finite difference formulation. The first well known document of this numerical technique was published by Evans and Harlow [61] at Los Alamos scientific laboratory. The advantages of FVM are low memory usage, low calculation time for many flow situations, the physical quantities conserve even on the coarse grids, etc. Accordingly, the FVM has become a favorite numerical technique for solving fluid flow problems.

For jet mixing tank modeling, the commercial and in-house CFD codes were adopted to simulate jet mixing tank. Most researchers selected the FVM as a numerical solution technique to study the jet mixing. For commercial CFD codes, Jayanti and Pavithra [62] employed commercial CFD code PHOENICS to study the hydro-

dynamics for dissolution of solids in liquid. Jayanti [38] studied the mixing of a soluble salt by using CFX commercial code and found that a tank with conical bottom minimized the dead zones. Breisacher and Moder [63] studied the jet mixing tanks of different scales by using FLOW-3D commercial CFD code with free surface simulation.

The most widely used finite volume commercial CFD code for jet mixing tank modeling was FLUENT. It was adopted to simulate the different jet mixing tank geometries. For a cylindrical tank with side entry jet, FLUENT was used to study the mixing performance enhancement by alternating jet [37] and to identify unacceptable flow pattern predictions by using the concept of residence time distribution (RTD) [64]. It was also used to investigate the effects of jet arrangement, such as jet angle, jet elevation, etc. [40-42], tank shape [55], jet injection rate [65], and types of fluid [66] on flow pattern and mixing performance for the inclined side entry jet mixing tank. Wasewar and Sarathi [67] and Bumrungthaichaichan et al. [68] also studied the jet mixing phenomena inside the inclined side entry jet mixed tank by using FLUENT.

Mathpati et al. [69] employed FLUENT to investigate the mean flow and turbulence quantities inside the jet loop reactor by using standard k-epsilon model (SKE), Reynolds stress model (RSM), and large eddy simulation (LES). Dautova et al. [70] also simulated the axial jet mixing tank by using FLUENT with different turbulence models, including Spalart-Allmaras (SA), RSM, shear stress transport (SST) k-omega, and k-omega transient turbulence models. They showed that the predicted results of k-omega transient turbulence model showed the best agreement with PIV data as compared with other models. FLUENT was used to study the effect of jet angle in axial jet mixed tank as reported by Rafiei et al. [71]. The commercial CFD code FLUENT was also used to study the flow pattern and mixing performance inside cubic jet mixing tank [72], jet mixing tank with cooling coils [73,74], as well as a tank with multiple jets [75,76].

A few researchers used FEM to simulate jet mixing. Egedy et al. [77] simulated jet mixers with different numbers of jet holes by using COMSOL with coarse tetrahedral grids. The results revealed that, for residence time, qualitative similarities between the measurement and the simulated results were achieved, meaning that the only tendency of the predicted residence time was similar to the experimental data.

For in-house CFD codes, Patwardhan [39] developed the finite volume in house CFD code to simulate the inclined side entry jet mixing tank. The governing equations were discretized by control volume formulation on a staggered grid arrangement [27]. He showed that his CFD code can be used to simulate the inclined jet mixing tanks. Thatte et al. [53] used the in-house CFD code, which was similar to Patwardhan [39], to simulate axial jet mixing tank. The results revealed that the predicted residence times agreed well with radiotracer experimental data.

Rahimi and Parvareh [54] used in-house finite volume CFD code to investigate the different jet nozzle angles in a semi-industrial stirred tank. The results showed that the tank with a nozzle angle of 45^{o} showed the minimum mixing time. Marek et al. [78] employed the in-house CFD code, which was developed originally in Bristol University and validated on a large variety of open-channel flow situations [79], to obtain a flexible CFD modeling for the design and optimization of water storage tanks, including the effects of varying water depths and density stratification. The results revealed that the CFD model predicted the overall mixing time well. However, the normalized concentration profiles were not in good agreement with experimental data. These incorrect normalized concentration profiles were improved by using higher order convection scheme.

As mentioned, the FVM and FEM can be used to simulate jet mixing tanks. To achieve accurate predicted results, the CFD code should be confirmed that it is suitable for solving the non-self adjoint PDEs, especially for the FEM CFD code. In other words, if the CFD code is developed by using GFEM, the obtained results may not represent the physical flow features.

2. Turbulence Modeling for Jet Mixing Tanks

Turbulent flow is a flow region characterized by chaotic property changes. This includes rapid variation of pressure and velocity in space and time (highly unsteady state), rapid mixing due to diffusivity, three-dimensional flow, rotational flow structures (turbulent eddies, including small and large eddies), and high Reynolds number. Turbulent flow is dissipative, meaning that the kinetic energy gets converted into heat due to viscous shear stresses. An important characteristic which makes the deterministic approach to turbulence problems impossible is irregularity (randomness). So, the turbulent flows are usually described by statistical approach.

Turbulent flow problems can be resolved by several ways. Direct numerical simulation (DNS) directly resolves all turbulent eddies, which requires a powerful computing facility. The less accurate way to resolve the turbulence is large eddy simulation (LES), which only solves the large turbulent eddies while the small scale eddies are modeled. In engineering applications, it is unnecessary to resolve the details of the turbulent fluctuations, so only the effects of turbulence on the mean flow are considered. The mean flow properties can be calculated by turbulence model, which is based on the time-averaged Navier-Stokes equations [80]. Over nine decades, many turbulence models have been developed, such as Prandtl mixing length model, k-epsilon model, and k-omega model.

For a jet mixing tank, the flow pattern inside the tanks is always turbulent flow. So, the turbulence calculations of the jet mixing tanks are necessary. Many researchers studied the effect of turbulence models on jet mixing tank simulations. Zughbi and Rakib [40] used SKE and RSM turbulence models to predict the turbulence inside the tanks. The results showed that the difference in final mixing times of these models was less than 1% and the calculation time of RSM was about three-times higher than SKE. Then, the SKE was selected to study their jet mixing tanks. Many researchers showed that it was successfully adopted to predict the overall mixing time [39,42]. However, the predicted concentration profiles of SKE were not in good agreement with experimental data.

Rahimi and Parvareh [54] studied the jet mixing tank by using three different types of k-epsilon model, including SKE, renormalization group k-epsilon model (RNGKE), and realizable k-epsilon model (RKE). The overall mixing times predicted by RNGKE exhibited better results as compared with other k-epsilon models. Zughbi and Ahmad [41] studied inclined side entry jet mixing tanks. The simulations involved using four different turbulence

models: SKE, RNGKE, RKE, and RSM. The simulated results were similar to Zughbi and Rakib [40] that the SKE was the suitable turbulence model because of the accuracy in mixing time prediction and its calculation time. Marek et al. [78] employed k-epsilon and k-omega turbulence models to study the inclined side entry jet mixing tanks. However, the discussion about these models was not expressed.

Mathpati et al. [69] investigated the mean and turbulence quantities in jet loop reactor by using SKE, RSM, and LES. The results revealed that the RSM and LES gave better agreement with PIV data as compared to SKE, that showed the overprediction in turbulence production and transport as comparison with those estimated by LES. Furman and Stegowski [64] employed three different models, including SKE, RNGKE, and RSM, to study the side entry jet mixing tanks. The results indicated good agreement in mean residence time between RNGKE and experimental data was achieved. For qualitative analysis, the predicted path lines of RNGKE were acceptable as compared to the experimental flow visualization.

Dautova et al. [70] assessed the performance of SA, RSM, SST k-omega, and k-omega transient turbulence models by comparing with the data obtained by PIV data, including radial and axial velocities, in axial jet mixing tanks. The results revealed that RSM was slightly better in axial velocity and SST k-omega was much better in radial velocity. The SA model exhibited poor predictions in both axial and radial velocities as compared with the other models. The transient mode of k-omega model showed smooth convergence, meaning that the balance of the conservation equations was achieved. Finally, they concluded that the velocity profiles predicted by k-omega transient model produced the best agreement with experimental data as compared to the other models.

For turbulence model selection, most researchers showed that the SKE was a suitable model for predicting the fluid flow in jet mixing tanks. However, it contradicts the suggestion that the SKE is not suitable for round jet simulation. There is no universal turbulence model that can be used to simulate all turbulent flow situations. So, researchers must carefully select the turbulence model by considering the results predicted by different turbulence models for their jet mixing tank configurations before other parametric studies.

3. Boundary Conditions Setup

For jet mixing tank simulations, the appropriate boundary conditions are specified at four different general tank boundaries, including inlet, outlet, top surface, and wall. At inlet section, the value of velocity [38,39,42,67,68,70,72,76,78] or velocity profile [69] or mass flow rate [64] can be specified. To solve turbulent flow inside the tank, the turbulence intensity was also specified at inlet section [39,68,70]. Patwardhan [39] suggested that a turbulence intensity of 10% showed a better match with experimental data as compared to the other turbulence intensity values. Bumrungthaichaichan et al. [68] also specified a turbulence intensity of 10% at jet inlet. Dautova et al. [70] used an experimental turbulence intensity of 4.7% as a turbulence boundary condition. Furthermore, the momentum source can be used to create the water flow through the jet nozzle [40,41,65], meaning that the jet velocity is introduced.

For outlet section, the outflow boundary condition was commonly used to simulate jet mixing tanks [70,72,76,78]. The mass flow rate [38,67] or pressure outlet [68] can also be imposed as an outlet boundary condition. At the wall, most researchers used no-slip boundary condition with standard wall function to solve the near wall flow. For temperature tracer technique simulation, the zero heat flux was adopted at the wall [41,67]. At top boundary, the flat interface was commonly assumed by using symmetry boundary condition, i.e., the normal flux and the gradients of all variables were specified to be zero, for computational efficiency [39,68,69, 74,75,78]. For free surface simulation, the volume of fluid (VOF) method was employed. Then, the applied pressure on the surface of the tank was specified [72].

4. Numerical Methods

4-1. Pressure-velocity Coupling Schemes

The pressure-velocity coupling iterative solution strategy was presented to resolve two important problems: the non-linear quantities in momentum equations and the absence of transport equation for pressure [28]. Pressure-velocity coupling algorithms are used to derive the pressure equations from the continuity and momentum equations. Many researchers employed the most famous SIMPLE algorithm of Patankar and Spalding [81], which stands for semi-implicit method for pressure-linked equations, to simulate jet mixing tanks [42,54,68,72,78]. This algorithm was originally a guess-and-correct procedure for pressure calculation on staggered grid arrangement. The pressure correction equation, which is derived from discretized continuity and momentum equations, is used to obtain the correct pressure and velocity fields.

Patwardhan [39] used SIMPLER (SIMPLE Revised) algorithm, which is an improved version of SIMPLE, to simulate inclined side entry jet mixed tanks. This algorithm adopts the discretized equation for pressure to achieve the pressure field instead of a pressure correction equation as in SIMPLE, meaning that the pressure field is directly obtained without the use of correction. The simulated results showed that this algorithm was successfully adopted to predict the overall jet mixing time.

The PISO (pressure-implicit with splitting of operators), which is based on a higher degree of the approximate relation between the corrections for pressure and velocity, was also successfully used to simulate inclined side entry jet mixing tanks [40,65,67] and jet loop reactor [69]. This algorithm is a part of the SIMPLE family. It improves the computational efficiency as compared to SIMPLE by performing the two additional corrections, including neighbor and skewness corrections. This algorithm is recommended for transient calculations [82]. Wasewar and Sarathi [67] suggested that both PISO and SIMPLE exhibited the same results for steady state problems. However, the computational time of SIMPLE was lesser than PISO.

As mentioned, for jet mixing tank simulations, SIMPLE and PISO are suitable algorithms for steady state and transient simulations, respectively. Generally, the PISO is recommended for all transient flow simulations. Furthermore, a stable calculation with a large time step size and a large under relaxation factor (URF) is achieved by using PISO. However, for unsteady state simulation with small time step size, the PISO may increase the computational cost, so the SIMPLE or other algorithms should be considered instead. Hence, before performing the transient simulation of jet mixing tank, it is a good practice to consider the algorithm by using the

time step size.

4-2. Spatial Discretization Scheme

Generally, the values of scalar variable (ϕ) are stored at the center of cells. However, the face values of scalar variable (ϕ_f) are required for the convection terms in discretized transport equation of scalar variable and must be interpolated by using cell center values [83]. It is commonly accomplished by using an upwind scheme, meaning that the face value is derived from the quantities in the upstream or upwind cell. For jet mixing tank simulations, different discretization schemes, such as first-order upwind and second-order upwind, were used to interpolate the face values.

The simplest upwind scheme is first-order upwind (FOU), which is a first-order accuracy scheme. For FOU, the face values are identical to the cell center values of upwind cells. The jet mixing tank modeling can be carried out by using FOU scheme. Ranade [37] employed SKE with FOU scheme to reduce CPU requirements for side entry jet mixing tank simulations. Rahimi and Parvareh [54] numerically studied the side entry jet mixing tanks by using in house finite volume CFD code. The FOU was employed to estimate all variables, except the pressure. The pressure was discretized by standard scheme. Further, Parvareh et al. [72] adopted standard scheme for pressure and FOU for all variables to simulate the cubic jet mixed tanks.

The second discretization scheme for jet mixing tank modeling is the power law, which interpolates the face value by using the analytical solution of the one-dimensional convection-diffusion equation [83]. Patwardhan [39] developed his CFD code with power law discretization scheme to study the inclined side entry jet mixing tanks. Further, Raja et al. [55] and Wasewar and Sarathi [67] also used power law scheme for the inclined side entry jet mixing tank simulations.

The higher order upwind scheme was also employed to study jet mixing tanks. Jayanti [38] investigated the cylindrical jet mixing tanks with different bottom shapes by using higher upwind scheme or CONDIF scheme. Marek et al. [78] simulated the inclined side entry jet mixed tanks. Convective and diffusive fluxes were approximated by applying the first/second-order accuracy hybrid differencing scheme or the second-order accuracy HLPA differencing scheme [84]. Mathpati et al. [69] numerically studied the jet loop reactor by using QUICK (Quadratic upwind interpolation for convective kinetics) for RANS-based turbulence model and bounded central difference scheme for LES. Breisacher and Moder [63] used second-order advection scheme to numerically study the jet mixing tanks with different scales. Jaiklom et al. [42] studied the inclined side entry jet mixing tanks and used second-order upwind (SOU) scheme, which computes the face values by using a multidimensional linear reconstruction approach [85], to interpolate the momentum and tracer. The pressure and turbulence quantities were estimated by standard and FOU, respectively. Bumrungthaichaichan et al. [68] used standard and SOU to interpolate the pressure and other variables, respectively. They showed that the accuracy of concentration profile prediction can be improved by using the fine mesh and SOU scheme.

As mentioned, the various spatial discretization schemes were successfully adopted to simulate the different jet mixing tanks. However, these schemes may promote numerical diffusion [86], which is an error that always occurs in CFD, especially for FOU. The numerical diffusion shows itself as equivalent to an increase in diffusion coefficient, e.g., viscosity for momentum equations, thermal conductivity for energy equation, etc. For jet mixing tank simulations, in order to minimize the numerical diffusion, the higher order spatial discretization schemes, such as SOU, QUICK, are recommended.

4-3. Temporal Discretization Scheme

In transient simulation, the governing equations are discretized in both space and time. Temporal discretization is obtained by integrating every term in the differential equations over a time step (Δt). For jet mixed tank modeling, the unsteady state simulation is required to investigate the mixing time. However, there are a few reports about the temporal discretization scheme in jet mixing tank simulations. Patwardhan [39] investigated the mixing times for inclined side entry jet mixing tanks by using implicit method. Marek et al. [78] selected the second-order implicit scheme to discretize the governing equations of their inclined side entry jet mixing tanks. Mathpati et al. [69] also used the second-order implicit scheme with time step size of 0.0005 s for LES of jet loop reactor. Further, Bumrungthaichaichan et al. [68] adopted the first-order implicit to investigate the mixing inside the inclined side entry jet mixing tank.

For jet mixing tank simulations, the proper spatial discretization scheme is employed to obtain the accurate flow patterns. The concentration (or temperature) distributions and mixing time should also be achieved by using the suitable temporal discretization scheme. According to the previous reports, the proper temporal discretization schemes for SKE and LES were first-order implicit and second-order implicit, respectively. However, as mentioned, the reports of the temporal discretization scheme are less than the information of spatial discretization scheme. To achieve the proper temporal discretization scheme for jet mixing tank modeling, the concentration (or temperature) distribution should be initially simulated by using the first-order implicit solver. Moreover, the second-order implicit solver should be used instead for the same unsteady simulation. Then, the concentration (or temperature) profiles obtained by these two different solvers must be compared.

5. Solution Strategy

5-1. Simulation Procedure

For jet mixing tank modeling, many researchers suggested that the simulation procedure can be separated into two main parts [38,54,55,66,68,72]. In the first part, the velocity field was obtained by using steady state simulation for the given geometry and boundary conditions. This velocity field was then used as an initial velocity field for the transient simulation. In the second part, the tracer was patched or injected into the tank. Then, the unsteady state simulation was carried out to obtain the concentration (or temperature) distribution inside the tank, which was used to identify the mixing time.

5-2. Time Step Size for Transient Calculation

Unsteady state simulations are required to investigate the jet mixing times. For transient simulation, the time step size must be specified. The time step can be constant or gradually increased from the initial time step size. The effect of time step size on the numerical solutions should be studied before other parametric studies. Ranade [37] showed that the reduction of time step size below 0.05 s had no significant effect on the predicted mixing time. So, the time

step of 0.05 s was selected for all mixing simulations. Jayanti [38] used a time step of 0.02 s for concentration distribution simulations. This initial time step size was gradually increased to the maximum of 0.05 or 1 s for the large values of time depending on the case being tested. Patwardhan [39] used the transient simulations with the initial dimensionless time step of 0.0025, which was slowly increased to 0.25, to obtain the concentration fields inside the tanks.

Zughbi and Rakib [40] and Zughbi and Ahmad [41] showed that the time step of 1 s was sufficient to use in the transient simulations. Raja et al. [55] simulated the concentration field by using time step of 0.05 s, which was increased gradually to the maximum time step of 1 s. Sendilkumar et al. [66] started the unsteady state simulation with time step of 0.1 s and slowly extended the time step to the maximum value of 1 s. Wasewar and Sarathi [67] initially simulated the temperature distributions inside the jet mixing tanks by using time step of 1 s. The initial time step was slowly increased to 0.5 s, 1 s, 2 s, 5 s and finally 10 s. Mathpati et al. [69] studied the jet loop reactor by LES with the time increment of 0.0005 s. Parvareh et al. [72] investigated the tracer concentration distributions inside the cubic tanks by using unsteady simulation with a constant time step of 0.01 s. Further, Bumrungthaichaichan et al. [68] used the time step size of 0.0025 s to eliminate any uncertainty in jet mixing time prediction.

According to previous reports, the selected time step sizes of jet mixing tank simulations were obtained by trial and error method. In other words, the different time step sizes were simulated and compared to achieve the optimal time step size, which presents a small variation in predicted results (e.g., concentration profiles, mixing time, etc.) as compared to the smaller time step sizes. This trial and error method is sometimes suitable for dealing with specific problem. Generally, the time step is a function of flow condition and physical geometry. To obtain the proper time step size by using the flow condition and physical geometry, the appropriate length and velocity scale approach or Courant-Friedrichs-Lewy (CFL) condition [87] approach should be considered. The CFL condition is a condition in numerical equation solving which uses to consider a proper time step size that prevent the numerical instability.

The time step sizes obtained by the two latter methods can be demonstrated by considering a simple jet mixing tank modeling. The simple model is a vertical cylindrical tank. The inclined nozzle is inserted into the tank bottom. The jet with a velocity of 4.4 m/s diagonally flows through the tank and hit the opposite boundary. The distance between nozzle exit and opposite boundary is 0.65 m. For appropriate length and velocity scale approach, the time step size is given by

$$\Delta t = \frac{1}{N}\frac{L}{U} \tag{7}$$

where N is number of iterations per time step ($10 \le N \le 200$), L is length scale, and U is velocity scale. For this simple mixing tank, the distance between nozzle exit and opposite boundary and jet exit velocity are considered as length scale and velocity scale, respectively. If N=20, the time step size for this simple jet mixing tank is

$$\Delta t = \frac{1}{20}\frac{0.65\ \text{m}}{4.4\ \text{m/s}} = 0.007386\ \text{s} \tag{8}$$

For CFL condition approach, the time step size is evaluated by considering the Courant number (C). The Courant number is defined as

$$C = \frac{U\Delta t}{\Delta x} \le C_{max} \tag{9}$$

where U is velocity scale and Δx is grid size. The value of C_{max} is the maximum Courant number, which is dependent on the solver method. For explicit solvers, the value of C_{max} is 1. Typically, the implicit solvers are less sensitive to numerical instability as compared to the explicit method. So, the value of C_{max} can be larger than 1. For this simple jet mixing tank, the distance between nozzle exit and opposite boundary is equally divided into 100 cells. So, the time step size of a simple jet mixing tank for the Courant number of unity is

$$\Delta t = \frac{\Delta x}{U} = \frac{0.65\ \text{m}/100}{4.4\ \text{m/s}} = 0.001477\ \text{s} \tag{10}$$

From these two latter methods, the time step size is dependent on jet mixing tank geometry, jet velocity (Reynolds number), and mesh size. The computed time step sizes of these methods are smaller than that reported by previous works. So, the computational times of these time step sizes should be larger than the trial and error method. The higher time step sizes of trial and error method can be adopted for implicit solver only. For jet mixing tank simulations, in order to obtain the accurate results and high computational stability, the CFL condition approach is recommended. The trial and error method is adopted to achieve a fast computational time. So, the researchers should carefully consider the proper time step size before performing their jet mixing tank simulations.

5-3. Convergence Criteria

For iterative solver, the calculation process is repeated until the change in the variable from one iteration to the next becomes small. So, the results are considered as converged solutions. At the convergence, all discretized transport equations are obeyed to a specified tolerance in all cells and the solution no longer changes with additional iterations. Moreover, the mass, momentum, energy, and scalar balances are achieved. Generally, scaled residuals are adopted to identify the convergence. For jet mixing tank modeling, many researchers used the scaled residuals as the convergence criterion. The difference between the concentration and well mixed concentration at all points inside the tank was also conducted as a convergence criterion.

Ranade [37] reported that the computations were carried out until the normalized residue of species equation was below 0.001. Patwardhan [39] specified the normalized mass residue of 0.005 as a convergence criterion. Rahimi and Parvareh [54] showed that the jet mixing tank simulations were carried out by using a residual below 0.001. Mathpati et al. [69] simulated the jet loop reactor by using RANS turbulence models and LES. The residual for turbulence models was below 0.0001. For LES, the jet loop reactor was simulated by using 40,000 time steps. Parvareh et al. [72] selected a residual below 10^{-7} as the convergence criterion for cubic jet mixing tank simulations. Bumrungthaichaichan et al. [68] achieved accurate results for inclined side entry jet mixing tank simulations

by using a residual below 10^{-5}. For temperature tracer technique, most researchers suggested that the residuals for energy and other variables should fall below 10^{-6} and 0.001, respectively [40,66,67].

For other convergence criteria, the tracer concentrations were used to indicate the solution convergence. Jayanti [39] and Raja et al. [55] simulated the jet mixing tank until the concentration at all points differed by less than 0.1% from the fully mixed concentration. Lee and Armstrong [73] and Leishear et al. [75] considered that the solutions were converged when the tracer concentrations at all points inside the tanks reached the 95% of well mixed concentration. Lee [74] performed simulations of the jet mixing tanks until the species concentrations were reached at equilibrium concentration within 1% relative error.

According to the previous reports, most researchers used the residual to consider the solution convergence. For residual convergence criterion, the low residuals do not mean correct results, and high residuals do not show a wrong solution. To obtain converged results, it is a good practice to perform the calculation until the all residuals no longer change. Other convergence monitors, such as the velocity magnitude at outlet of jet mixing tank, should be included to consider the solution convergence. Thus, converged results can be achieved when the other monitors no longer change.

6. CFD Grid

In conventional CFD simulation, the computational domain is discretized into a set of non overlapping grids (meshes). This process is called grid generation (or meshing). There are many grid types in CFD simulation. For two-dimensional domain the two different grid types, including triangular and quadrilateral grids, are commonly used. In three-dimensional simulation, the several grid types are available, such as tetrahedron, hexahedron, and polyhedron, The grid has a significant impact on convergence rate, computational time, and solution accuracy. Generally, the simulated results should be independent on the number of grids, meaning that the solutions no longer change while the number of grids is increased. These obtained results are known as grid independent solutions.

For CFD modeling of jet mixing tanks, different meshing schemes were used, including body-fitted grid, tetrahedron, hexahedron, polyhedron, and hybrid (the combination between tetrahedron and hexahedron). Ranade [37] simulated the side entry jet mixing tanks by using the body-fitted grid with 60,648 cells. Jayanti [38] employed 3,600-6,000 non-uniform grids to study jet mixing tanks with different bottom shapes. Furman and Stegowski [64] used 59,000 hexahedral grid cells to study flow pattern inside cylindrical side entry jet mixing tanks.

Patwardhan [39] employed in-house CFD code with 216,000 nodes, which were grid independent solutions, to investigate the mixing phenomena inside inclined side entry jet mixing tanks. Raja et al. [55] simulated inclined side entry jet mixed tanks by using 125,000 nodes (grid independent solutions). For inclined side entry jet mixing tank simulations, most researchers used tetrahedral grid generation scheme because it is easy to generate the grids at an acute angle between jet nozzle and tank wall. Zughbi and Rakib [40,65] adopted 45,484 and 46,829 tetrahedral cells for their studies. Rahimi and Parvareh [54] simulated the inclined side entry jet mixing tanks by using 600,000 tetrahedral cells.

Zughbi and Ahmad [41] generated tetrahedral grids to simulate the inclined side entry jet mixing tanks with symmetric jet and asymmetric jet, respectively. Grid independent solutions were, respectively, achieved by using 116,186 and 252,801 cells for symmetric jet and asymmetric jet. Sendilkumar et al. [66] numerically studied the mixing characteristics for Newtonian and non-Newtonian fluids inside the inclined side entry jet mixing tanks by using 130,900 tetrahedral cells. Wasewar and Sarathi [67] employed 50,000-80,000 tetrahedral cells to study the jet mixing phenomena. Muhammad and Kizito [76] studied the single and dual side entry jet mixing tanks by using tetrahedral grid. Grid independent solutions were obtained by using the grid with interval size of 15 mm. Moreover, the tetrahedral grid can also be adopted to simulate the inclined side entry jet for cubic mixing tank as reported by Parvareh et al. [72].

For hexahedral grid, Marek et al. [78] generated the hexahedral grid with 900,000 nodes inside the inclined side entry jet mixing tanks to investigate the effects of jet velocity, nozzle diameter and nozzle angle on jet mixing performance. Jaiklom et al. [42] used the CFD models with 1,007,780 hexahedral cells to study the mixing time for free jet and wall jet inside the inclined side entry jet mixing tanks. Bumrungthaichaichan et al. [68] studied the effect of jet nozzle angle on mixing time for different liquid levels inside the inclined side entry jet mixing tanks by using hexahedral grid. They clearly demonstrated the investigation of grid-independent solutions by comparing the dimensionless axial velocity profiles along the jet centerline for different grid numbers as depicted in Fig. 5. The results showed that the model with 908,809 nodes was a grid-independent solution.

In axial jet mixing tank simulations, Mathpati et al. [69] used hexahedral grid to studied jet loop reactor. The number of hexahedral grids for RANS turbulence models and LES was 6×10^5 and 2.5×10^6 nodes, respectively. Breisacher and Moder [63] employed two-dimensional axisymmetric CFD models with 18,249 cells to study the axial jet mixing tanks. Dautova et al. [70] investigated the flow patterns inside the symmetric axial jet and asymmetric

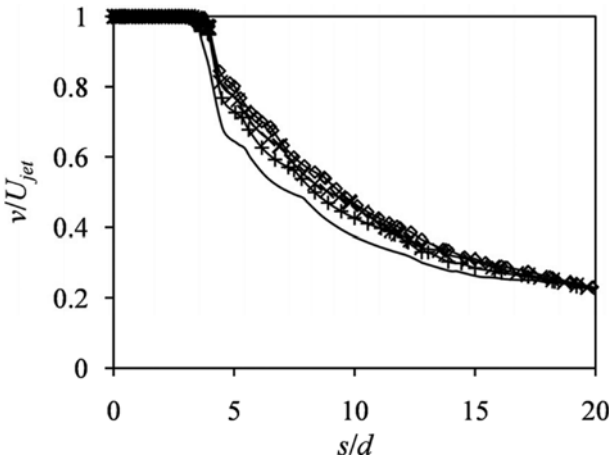

Fig. 5. The dimensionless axial velocity profiles along the jet centerline for different grid numbers from Bumrungthaichaichan et al. [68]: — 680,997 nodes; –+– 737,707 nodes; –×– 908,809 nodes; –◇– 1,110,432 nodes.

Table 2. Summary of numerical setup for jet mixing tank simulations

Authors	Geometry	Numerical technique	Grid generation	Turbulence models	P-V coupling scheme / Interpolation scheme	Temporal discretisation scheme / Time step size	Convergence criteria
Ranade (1996)	Cylindrical tank with side entry jet	FVM (FLUENT)	Body-fitted grid with 60,648 cells	SKE	Not mentioned / FOU	Not mentioned / 0.05 s	Normalized residue of species equation $<10^{-3}$
Jayanti (2001)	Cylindrical jet mixing tank	FVM (CFX)	Non-uniform grid with 3,600-6,000 cells	RNGKE	Not mentioned / Higher upwind scheme or CONDIF scheme	Not mentioned / 0.02 s (Gradually increased to 0.05 s or 0.1 s)	The equations were solved until the concentration at all points differed by less than 0.1% from the fully mixed value
Patwardhan (2002)	Cylindrical tank with inclined side entry jet	FVM (In house)	216,000 nodes	SKE	SIMPLER / Power law	Not mentioned / Dimensionless time step of 0.0025 (Gradually increased to 0.25)	Normalized mass residue <0.005
Zughbi and Rakib (2002)	Cylindrical tank with inclined side entry jet	FVM (FLUENT)	Tetrahedral grid with 45,484 cells	SKE	PISO / Not mentioned	Not mentioned	Not mentioned
Thatte et al. (2004)	Cylindrical tank with axial jet	FVM (In house)	Not mentioned	Same as Patwardhan (2002)			
Zughbi and Rakib (2004)	Cylindrical tank with inclined side entry jet	FVM (FLUENT)	Tetrahedral grid with 46,829 cells	SKE and RSM	PISO / Not mentioned	Not mentioned / 1 s	Residual $<10^{-3}$ for all variables and $<10^{-6}$ for energy
Rahimi and Parvareh (2005)	Cylindrical tank with inclined side entry jet	FVM (In house)	Tetrahedral grid with 600,000 cells	SKE, RNGKE, and RKE	SIMPLE / Standard for pressure and FOU for other quantities	Not mentioned	Residual $<10^{-3}$
Zughbi and Ahmad (2005)	Cylindrical tank with inclined side entry jet	FVM (FLUENT)	Tetrahedral grid with 116,186 cells for symmetric jet model and 252,801 cells for asymmetric jet model	SKE, RNGKE, RKE, and RSM	Not mentioned	Not mentioned / 1 s for symmetric jet model and asymmetric jet model	Not mentioned
Marek et al. (2007)	Cylindrical tank with inclined side entry jet	FVM (In house)	Hexahedral grid with 900,000 nodes	k-epsilon and k-omega	SIMPLE / First/second order hybrid scheme or second order HLPA scheme	Second order implicit / Not mentioned	Not mentioned
Raja et al. (2007)	Cylindrical tank with inclined side entry jet	FVM (FLUENT)	125,000 nodes	SKE	Not mentioned / Power law	Not mentioned / 0.05 s (Gradually increased to 0.1 s)	The equations were solved until the concentration at all points differed by less than 0.1% from the fully mixed value

Table 2. Continued

Authors	Geometry	Numerical technique	Grid generation	Turbulence models	P-V coupling scheme / Interpolation scheme	Temporal discretisation scheme / Time step size	Convergence criteria
Sendilkumar et al. (2007)	Cylindrical tank with inclined side entry jet	FVM (FLUENT)	Tetrahedral grid with 130,900 cells	RNGKE	Not mentioned / Higher order upwind scheme	Not mentioned / 0.1 s (Gradually increased to 1 s)	Residual $<10^{-3}$ for all variables and $<10^{-6}$ for energy
Wasewar and Sarathi (2008)	Cylindrical tank with inclined side entry jet	FVM (FLUENT)	Tetrahedral grid with 50,000-80,000 cells	SKE	SIMPLE for steady state and PISO for unsteady state / Power law for all variables and second order upwind for energy	Not mentioned / 0.1 s (Gradually increased to 0.5 s, 1 s, 2 s, 5 s, and 10 s)	Residual $<10^{-3}$ for all variables and $<10^{-6}$ for energy
Mathpati et al. (2009)	Cylindrical tank with axial jet (jet loop reactor)	FVM (FLUENT)	Hexahedral grids with 600,000 nodes for RANS turbulence models and 2.5 million nodes for LES	SKE, RSM, and LES	PISO / QUICK for RANS turbulence model and bounded central difference scheme for LES	Second order implicit / 0.0005 s for LES	Residual $<10^{-4}$ for RANS turbulence model and 40,000 number of time steps for LES
Parvareh et al. (2009)	Cubic vessel with a volume of 125 liters	FVM (FLUENT)	Tetrahedral grid with 687,342- 713,170 cells	RNGKE	SIMPLE / Standard for pressure and FOU for other quantities	Not mentioned / 0.01 s	Residual $<10^{-7}$
Breisacher and Moder (2010)	Axial jet mixing tank	FVM (FLOW-3D)	18,249 cells (2D axisymmetric grids)	k-epsilon	Not mentioned / Second order advection scheme	Not mentioned	Not mentioned
Furman and Stegowski (2011)	Cylindrical tank with side entry jet	FVM (FLUENT)	Hexahedral grid with 59,000 cells	SKE, RNGKE, and RSM	Not mentioned	Not mentioned	Not mentioned
Lee and Armstrong (2011)	Jet mixing tanks with and without cooling coils	FVM (FLUENT)	Hybrid grid with 1×10^6 nodes for the tank without cooling coils and 4×10^6 nodes for the tank with cooling coils	SKE	Not mentioned	Not mentioned	The equations were solved until the acid species concentrations at all points in the tank reached the 95% mixing criteria
Dautova et al. (2012)	Cylindrical tank with symmetric axial jet and asymmetric axial jet	FVM (FLUENT)	Polyhedral grid with 1.5×10^6 nodes	Spalart-Allmaras, RSM, SST k-omega, and k-omega transient model	Not mentioned	Not mentioned	Not mentioned

Table 2. Continued

Authors	Geometry	Numerical technique	Grid generation	Turbulence models	P-V coupling scheme / Interpolation scheme	Temporal discretisation scheme / Time step size	Convergence criteria
Leishear et al. (2012)	Cylindrical tank with dual opposing jets	FVM (FLUENT)	Hybrid grid with 1×10^6 nodes for the tank without cooling coils and 4×10^6 nodes for the tank with cooling coils	SKE	Not mentioned	Not mentioned	The equations were solved until the species concentrations at all points in the tank reached the 95% mixing criteria
Muhammad and Kizito (2012)	Cylindrical tank with single inclined jet and dual inclined jets	FVM (FLUENT)	Tetrahedral grid with 15 mm interval grid size	Not mentioned	Not mentioned	Not mentioned	Not mentioned
Rafiei et al. (2012)	Cylindrical tank with axial jet and inclined top entry jet	FVM (FLUENT)	Tetrahedral grid with 410,000 cells	RNGKE	Not mentioned	Not mentioned	Not mentioned
Jaiklom et al. (2013)	Cylindrical tank with inclined side entry jet	FVM (FLUENT)	Hexahedral grid with 1,007,780 cells	SKE	SIMPLE/ Standard for pressure, SOU for momentum and tracer, and FOU for turbulence quantities	Not mentioned	Not mentioned
Lee (2013)	Jet mixing tanks with cooling coils	FVM (FLUENT)	Hexahedral grid with 5×10^5 nodes for the tank with cooling coils and 6×10^5 nodes for the tank with cooling coils and support structure	SKE	Not mentioned	Not mentioned	The equations were solved until the species concentrations of tank were reached at equilibrium concentration within 1% relative error
Egedy (2014)	Jet mixer	FEM (COMSOL)	Tetrahedral grid	k-epsilon	Not mentioned	Not mentioned	Not mentioned
Bumrungthai chaichan et al. (2016)	Cylindrical tank with inclined side entry jet	FVM (FLUENT)	Hexahedral grid with 908,809 nodes	SKE	SIMPLE/ Standard for pressure, SOU for all variables	First order implicit / 0.0025 s	Residual $<10^{-5}$

axial jet mixing tanks by using a polyhedral grid of 1.5×10^6 nodes, which were grid-independent solutions. The tetrahedral grid can also be used to model the axial jet mixing tanks [71].

For jet mixing tanks with cooling coils, Lee and Armstrong [73] and Leishear et al. [75] used CFD to simulate the jet mixing tanks with and without cooling coils. The number of hybrid grids for the tank with and without cooling coils was 4×10^6 and 1×10^6 nodes, respectively. Lee [74] also simulated jet mixing tanks with cooling coils by using hybrid grid generation scheme. For the tank with cooling coils and the tank with cooling coils and support structure, the number of hybrid grids was 5×10^5 and 6×10^5 nodes, respectively. For jet mixer, Egedy [77] studied the number of jet nozzle holes by using tetrahedral grids. The grid independence study was tested by using four different grid levels, including coarser, coarse, normal, and finer. The coarse grid level was selected for the model calculation.

As mentioned, the CFD grid affects convergence rate, computational time, and solution accuracy. So, the CFD grid is another source of numerical error. For jet mixing tank simulations, the tetrahedral grid generation scheme was often used because it is easy to generate at acute angle of the inclined jet mixing tank. Generally, the grid topology has an impact on solution accuracy. The tetrahedral grids (tri grids) show a larger truncation error as compared to hexahedral grids (quad grids). For jet mixing tank simulations, in order to minimize the truncation error and numerical diffusion, the hexahedral grid, which is aligned with the flow direction, is recommended to generate inside the jet mixing tank.

7. Summary of Numerical Setup

The numerical setup for CFD simulations of various jet mixing tanks, including numerical solution techniques, turbulence modeling, boundary conditions, numerical methods, solution strategy, and CFD grid, can be summarized as shown in Table 2.

VALIDATION OF THE MODEL

Validation is one of the most important CFD simulation procedures, which represents the reliability of the model. It is defined as the process of determining the degree to which a model is an accurate representation of the real world from the perspective of intended uses of the model [88]. Generally, the model validation is directly achieved by comparing the simulated results, i.e., pressure profiles, velocity profiles, temperature profiles, etc., with the experimental data or analytical solutions. The overall quantities, such as particle collection efficiency, production yield, and overall mixing time, can also be adopted to validate the model.

For mixing tank simulations, typically, the model validations have been carried out by comparing the predicted overall mixing times with the experimental data or mixing time correlation. The concentration profile, temperature profile, and jet velocity profile can also be used to validate the models. One of the earliest validations of jet mixing tank modeling was by Brooker [36]. He showed 14% error in the overall mixing time prediction as compared to the experimental data. Patwardhan [39] clearly showed the model validation by comparing the predicted overall mixing times and normalized concentration profiles with his experimental data. The results revealed that good agreement between predicted overall mixing time and experimental data was achieved. However, the predicted concentration profiles were not in good agreement with experiments.

Parvareh et al. [72] used visual observation technique to study cubic jet mixing tanks. The dark Nigrosine distributions were recorded by a digital camera. The CFD technique was also used to study the tracer distribution inside the tanks. The results showed that the percent of the colored area at different regions for experiments and CFD models was slightly different (the error <15%). Furman and Stegowski [64] employed residence time distribution (RTD) concept to study the side entry jet mixing tanks. The simulated results were obtained by three different turbulence models, including SKE, RNGKE, and RSM. The results revealed that the RTD function predicted by RNGKE exhibited better agreement with the experimental data as compared to other models. Many researchers also successfully validated the jet mixing tank models by comparing the overall mixing times with their experimental data [41,53-55,66,71,75,77].

The comparison between CFD results and previous experimental results can also be used to obtain the model validation. Marek

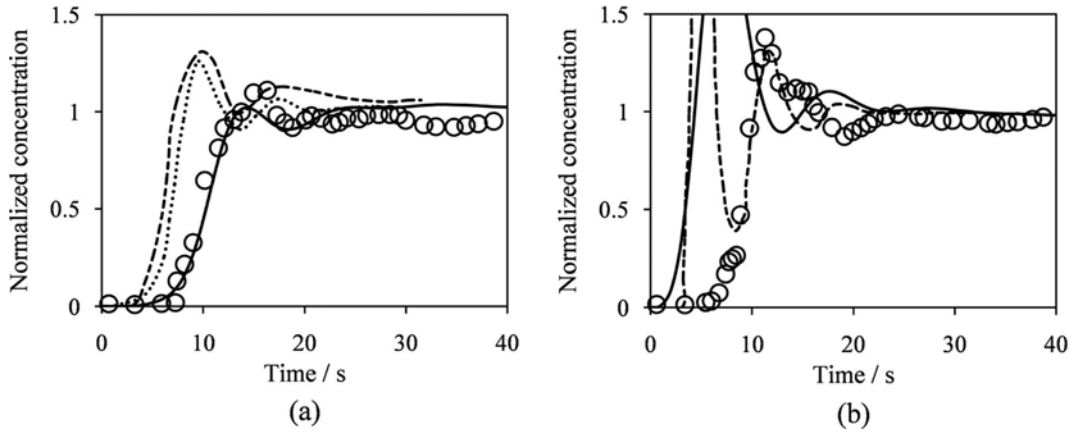

Fig. 6. Comparison between predicted normalized concentration and experimental data for 45° nozzle with 8 mm diameter and jet velocity of 4.4 m/s at (a) probe location 1 (b) probe location 2 from Bumrungthaichaichan et al. [68]: —— CFD; - - - CFD with standard constants [39]; ····· CFD with modified constants [39]; ○ Experiment [39].

et al. [78] and Bumrungthaichaichan et al. [68] compared their predicted normalized concentration profiles with the previous experimental data of Patwardhan [39]. Good agreement between CFD and experiment was achieved. Bumrungthaichaichan et al. [68] also revealed that the normalized concentration profile prediction could be improved by increasing number of nodes or decreasing the mesh size and using the second order upwind discretization scheme, especially for probe location 1, as shown in Fig. 6. Jaiklom et al. [42] successfully validated their simulated normalized concentration profiles by comparing with the previous experiment of Gaikwad [89]. Lee [74] simulated jet mixing tanks with cooling coils and compared the predicted results with the mixing time correlation of Grenville and Tilton [22] and the experimental data of Lee and Armstrong [73].

To achieve jet mixing tank model validations, the predicted overall mixing times can also be compared with the mixing time correlation. The various mixing time correlations were employed for model validations, including the correlations of Revill [2], Fossett and Prosser [6], Simon and Fonade [8], Fox and Gex [11], Lane and Rice [18], Maruyama et al. [19], and Grenville and Tilton [22]. The validation between predicted overall mixing time and mixing time correlations was originally reported by Ranade [37]. He compared the overall mixing time with the mixing time correlations of Revill [2] and Simon and Fonade [8]. The simulated results showed that his model seems to adequately capture the main features of fluid dynamics and mixing of jet mixing tanks.

Zughbi and Rakib [65] compared the predicted mixing time with correlation of Lane and Rice [18] to obtain model validation. Further, Zughbi and Rakib [40] extended their work and validated the inclined side entry jet mixing tank models by comparing with the mixing time correlations reported by Fossett and Prosser [6], Lane and Rice [18], and Grenville and Tilton [22]. The results showed that the predicted mixing times agree well with the correlation of Lane and Rice [18], and Grenville and Tilton [22]. However, the correlation of Fosset and Prosser [6] did not give a good agreement with their simulated results.

Furthermore, many researchers used the velocity profiles and temperature profiles to validate their models by comparing with their experimental measurements or the previous works. Mathpati et al. [69] experimentally studied the jet loop reactor and simulated this reactor by using SKE, RSM, and LES. The predicted results obtained by these three different simulations were compared with the PIV data. These simulations revealed that the flow in this reactor was different from the self-similar round jets. RSM and LES showed better agreement with PIV measurements as compared to SKE.

Breisacher and Moder [63] compared the predicted temperature profiles with the experimental measurements to achieve the model validation. The results showed that reasonable agreement between CFD and experimental data was achieved. Lee and Armstrong [73] validated their model by comparing jet velocity profile with the free jet correlation of Abramovich [90] and the previous data obtained by Kiser [91] and Post [92]. The results showed good agreement between simulated results and previous reports. Moreover, the predicted blending times were in good agreement with their tested results. Dautova et al. [70] also compared the predicted velocity profiles with PIV data to obtain model validation. The results showed that the velocity profiles achieved by k-omega transient model had the best agreement with the experimental data.

To demonstrate the higher reliability of the models, some researchers performed model validation by different aspects. Jayanti [38] used three different aspects to validate the jet mixing tank model. First, the predicted transverse velocity profiles were compared to the analytical solution of Schlichting [48]. The simulated jet spreading rate, i.e., the increase of jet width with distance, was validated by comparing with the result of White [93]. The jet spreading rate was represented by the ratio of jet width to the jet distance. The simulated ratio of jet width to the jet distance (0.191) was about 10% lower than the experimental data (0.212). Second, the calculated mixing times were compared with the correlation of Fox and Gex [11] for different jet Reynolds numbers. Finally, the normalized concentration profiles of Orfaniotis et al. [21] were adopted to compare with the simulated results. These results showed that the simulated results were fairly in good agreement with the previous reports. Wasewar and Sarathi [67] validated their model by comparing the predicted velocity fields with the analytical solution of Davies [47] and Schlichting [48]. Jet mixing times were also validated with the results obtained by Simon and Fonade [8], Lane and Rice [18], and Maruyama et al. [19]. The results revealed that good agreement between CFD modeling and previous results was observed.

According to these model validations, the CFD models successfully showed good agreement between predicted results and experimental data and/or analytical solutions. However, the measured velocity profiles inside the inclined jet mixing tanks were not adopted to validate the models, because such data are not available. To increase the model reliability, at least, the tendency of inclined jet velocity distribution for other flow situations, such as inclined dense jet [94] and inclined buoyant jet [95], should be conducted to compare with the predicted velocity profiles inside the jet mixing tank.

CONCLUSIONS

Computational fluid dynamics (CFD) was successfully employed to predict the various jet mixing tank configurations. The finite volume method is commonly used to simulate the jet mixing tanks. Many researchers showed that SKE was a suitable model for jet mixing tank simulations, especially for side entry and inclined side entry jet mixing tanks. For axial jet mixing tanks, the k-omega transient turbulence model or RSM or LES should be used instead of SKE. However, there is no universal turbulence model for all turbulent flow problems. So, the researchers must carefully test the capability of the selected turbulence model before other studies.

For numerical methods, the SIMPLE is a suitable algorithm for steady state simulation because of the calculation time efficiency. While, the PISO algorithm is prescribed for unsteady state simulation. The standard discretization scheme is commonly used to estimate the pressure. For other variables, the SOU is recommended to obtain the accurate normalized concentration profiles.

In transient simulations, the first-order and second-order implicit schemes are the appropriate temporal discretization schemes for

SKE and LES, respectively. To obtain accurate results and high computational stability, the CFL condition approach is recommended to consider time step size. At least, the different time step sizes must be tested until the solutions no longer change to achieve the proper time step size.

For convergence criteria, most researchers used the residual to decide the solution convergence. Generally, the residual for all variables and for energy should be less than 10^{-3} and 10^{-6}, respectively. The species concentrations can also be considered as a convergence criterion.

For grid generation, many CFD works showed that various meshing schemes were successfully employed to simulate jet mixing tanks. The tetrahedral grid generation scheme was the most commonly used to simulate inclined side entry jet mixing tank simulations because it is easy to generate the grids at the acute angle between the jet nozzle and tank wall. However, the grid-independence study must be tested to eliminate the numerical errors due to the coarseness of a grid before other studies.

For validation of the jet mixing tank model, generally, the overall mixing time and normalized concentration profile were used to compare with experimental data or mixing time correlation. The temperature profile and jet velocity profile can also be employed to validate the model. Due to the absence of measured velocity profiles inside the inclined jet mixing tank, at least, the tendency of the other inclined jet flow situations should be compared with the predicted velocity profiles of inclined jet mixing tank.

In future work, the effect of numerical methods on jet mixing tank modeling should be tested to achieve accurate results. For inclined side entry jet mixing tank, the model validation should be determined by comparing the simulated velocity profiles with the PIV experimental data.

NOMENCLATURE

Alphabetical Symbols

A : jet cross-sectional area
$b_{1/2}$: jet width
c^* : degree of mixing
C : Courant number
C_{max} : maximum Courant number
C_P : correlation constant of Fossett [1]
C_1, C_2 : correlation constant of Lane and Rice [17]
d_j : jet nozzle diameter
d_o : tank outlet diameter
D : tank diameter
f : mixing time factor for correlations of Fox and Gex [11] and Lane and Rice [18]
g : acceleration due to gravity
h_i : height of nozzle from bottom of tank
h_o : height of suction pipe from bottom of tank
H : height of liquid
J : jet momentum
J_s : specific jet momentum
k : correlation constant of Grenville and Tilton [24]
K : kinematic momentum
L : jet path length or length scale
M : mixing factor for correlation of Simon and Fonade [8]
N : number of iterations per time step
N_j : number of jets
Q : jet entrainment rate
Q_0 : jet efflux rate
r : radial distance of jet
Re_j : jet Reynolds number
t_{inj} : tracer injection time
t_m : mixing time
t_r : residence time
Δt : time step size
T^* : correlation constant of Hiby and Modigell [15]
u : jet axial velocity
u_c : jet centerline velocity
U : velocity scale
U_j : jet exit velocity
x : longitudinal or axial distance of jet
Δx : grid size

Greek Symbols

η : dimensionless variable for jet velocity profile correlation of Schlichting [48]
θ : jet nozzle angle
ν_0 : virtual kinematic viscosity
ρ : fluid density

REFERENCES

1. H. Fossett, *Chem. Eng. Res. Des.*, **29a**, 322 (1951).
2. B. K. Revill, in *Mixing in Process Industries*, N. Harnby, M. F. Edwards and A. W. Nienow Eds. Butterworth-Heinemann (1992).
3. D. Mewes and R. Renz, in *Seventh European Conference on Mixing*, Belgium, 131 (1991).
4. P. D. Hoffman, *AIChE Symp. Ser.*, **286**(88), 77 (1996).
5. R. Schimetzek, A. Steiff and P. M. Weinspach, *IChemE Symp. Ser.*, **136**, 391 (1995).
6. H. Fossett and L. E. Prosser, *Proc. I. Mech. E.*, **160**, 224 (1949).
7. J. A. Sarsten, *Pipeline and Gas J.*, **Sept.**, 37 (1972).
8. M. Simon and C. Fonade, *Can. J. Chem. Eng.*, **71**, 507 (1993).
9. J. Baldyga, J. R. Bourne and B. Zimmermann, *Chem. Eng. Sci.*, **49**, 1937 (1994).
10. N. Sudhindra and S. N. Sinha, in *Fourth European Conference on Mixing*, Netherlands, Paper C4 (1982).
11. E. A. Fox and V. E. Gex, *AIChE J.*, **2**, 539 (1956).
12. J. G. Van de Vusse, *Chemie. Ing. Tech.*, **31**, 583 (1959).
13. N. Okita and Y. Oyama, *Jpn. J. Chem. Eng.*, **27**, 252 (1963).
14. P. W. Coldrey, Paper to IChemE Course, University of Bradford, England (1978).
15. J. W. Hiby and M. Modigell, in *Sixth CHISA Congress*, Prague (1978).
16. I. H. Lehrer, *Chem. Eng. Res. Des.*, **59a**, 247 (1981).
17. A. G. C. Lane and P. Rice, in *International Chemical Engineering Symposium Series 64*, Paper K1 (1981).
18. A. G. C. Lane and P. Rice, *Chem. Eng. Res. Des.*, **60a**, 171 (1982).
19. T. Maruyama, Y. Ban and T. Mizushina, *J. Chem. Eng. Jpn.*, **15**, 342 (1982).

20. T. Maruyama, in *Encyclopedia of Fluid Mechanics Vol. 2*, N. P. Cheremisinoff Ed., Gulf Publishing Company (1986).
21. A. Orfaniotis, C. Fonade, M. Lalane and N. Doubrovine, *Can. J. Chem. Eng.*, **74**, 203 (1996).
22. R. K. Grenville and J. N. Tilton, *Chem. Eng. Res. Des.*, **74a**, 390 (1996).
23. R. K. Grenville, A. T. C. Mak and S. W. Ruszkowski, in *The 1992 IChemE Research Event*, 128 (1992).
24. R. K. Grenville and J. N. Tilton, in *Ninth European Conference on Mixing*, France, 67 (1997).
25. R. K. Grenville and J. N. Tilton, *Chem. Eng. Res. Des.*, **89**, 2501 (2011).
26. A. W. Patwardhan and S. G. Gaikwad, *Chem. Eng. Res. Des.*, **81**, 211 (2003).
27. S. V. Patankar, *Numerical Heat Transfer and Fluid Flow*, Hemisphere, New York (1980).
28. H. K. Versteeg and W. Malalasekera, *An Introduction to Computational Fluid Dynamics: The Finite Volume Method*, Addison Wesley Longman Ltd., England (1995).
29. J. D. Anderson Jr., *Computational Fluid Dynamics: The Basics with Applications*, McGraw-Hill, New York (1995).
30. G. Hetsroni, A. Mosyak, E. Pogrebnyak and L. P. Yarin, *Int. J. Heat Mass Tran.*, **48**, 1982 (2005).
31. P. Tongpun, E. Bumrungthaichaichan and S. Wattananusorn, *Songklanakarin J. Sci. Technol.*, **36**(4), 471 (2014).
32. A. W. Patwardhan and J. B. Joshi, *Ind. Eng. Chem. Res.*, **38**, 3131 (1999).
33. D. A. Deglon and C. J. Meyer, *Miner. Eng.*, **19**, 1059 (2006).
34. K. Elsayed and C. Lacor, *Appl. Math. Model.*, **35**, 1952 (2011).
35. K. Elsayed and C. Lacor, *Comput. Fluids*, **68**, 134 (2012).
36. L. Brooker, *Chem. Eng.*, **30**, 16 (1993).
37. V. V. Ranade, *Chem. Eng. Sci.*, **51**, 2637 (1996).
38. S. Jayanti, *Chem. Eng. Sci.*, **56**, 193 (2001).
39. A. W. Patwardhan, *Chem. Eng. Sci.*, **57**, 1307 (2002).
40. H. D. Zughbi and M. A. Rakib, *Chem. Eng. Sci.*, **59**, 829 (2004).
41. H. D. Zughbi and I. Ahmad, *Ind. Eng. Chem. Res.*, **44**, 1052 (2005).
42. N. Jaiklom, E. Bumrungthaichaichan and S. Wattananusorn, *Ladkrabang Eng. J.*, **30**(4), 37 (2013).
43. K. L. Wasewar, *Chem. Biochem. Eng. Q.*, **20**(1), 31 (2006).
44. C. G. Ball, H. Fellouah and A. Pollard, *Prog. Aerosp. Sci.*, **50**, 1 (2012).
45. X. Wang and S. K. Tan, *J. Hydrodyn.*, **22**(5), 1009 (2012).
46. J. K. Seok and W. S. Il, *Exp. Fluids.*, **38**, 801 (2005).
47. J. T. Davies, *Turbulence phenomena*, Academic Press, New York (1972).
48. H. Schlichting, *Boundary layer theory*, McGraw Hill, New York (1968).
49. M. L. Albertson, Y. B. Dai, R. A. Jensen and H. Rouse, *Trans. ASCE*, **115**, 639 (1950).
50. B. K. Revill, Paper to IChemE Course, University of Bradford, England (1981).
51. J. J. Perona, T. D. Hylton, E. L. Youngblood and R. L. Cummins, *Ind. Eng. Chem. Res.*, **38**, 1478 (1998).
52. A. G. C. Lane, *Liquid Jet Mixing in Tanks*, Ph.D. Dissertation, Department of Chemical Engineering, Loughborough University of Technology, Leicestershire, UK (1981).
53. A. R. Thatte, A. W. Patwardhan, H. J. Pant, V. K. Sharma, G. Singh and Ph. Berne, in *International Conference on Tracers and Tracing Methods*, Poland (2004).
54. M. Rahimi and A. Parvareh, *Chem. Eng. J.*, **115**, 85 (2005).
55. T. Raja, P. Kalaichelvi and N. Anantharaman, *J. Sci. Ind. Res.*, **66**, 522 (2007).
56. F. H. Harlow and J. E. Fromm, *Sci. Am.*, **212**(3), 104 (1965).
57. L. F. Richardson, *Philos. T. R. Soc. Lond.*, **210**, 307 (1911).
58. A. Thom, *Philos. T. R. Soc. Lond.*, **141**(845), 651 (1933).
59. B. H. Dennis and R. Kumar, in *ASME IDETC/CIE 2008*, Brooklyn, U.S.A. (2008).
60. R. Kumar and B. H. Dennis, in *ASME Early Career Technical Conference*, Arlington, U.S.A. (2009).
61. M. W. Evans and F. H. Harlow, *The particle-in-cell method for hydrodynamic calculations*, Los Alamos Scientific Laboratory, U.S.A. (1957).
62. S. Jayanti and J. Pavithra, in *International Conference on Advances in Chemical Engineering*, India, 125 (1996).
63. K. Breisacher and J. Moder, *Computational Fluid Dynamics (CFD) Simulations of Jet Mixing in Tanks of Different Scales*, NASA, U.S.A. (2010).
64. L. Furman and Z. Stegowski, *Chem. Eng. Process.*, **50**, 300 (2011).
65. H. D. Zughbi and M. A. Rakib, *Chem. Eng. Commun.*, **189**, 1038 (2002).
66. K. Sendilkumar, P. Kalaichelvi, M. Perumalsamy, A. Arunagiri and T. Raja, in *World Congress on Engineering and Computer Science 2007*, San Francisco, U.S.A. (2007).
67. K. L. Wasewar and J. V. Sarathi, *Eng. Appl. Comp. Fluid Mech.*, **2**(2), 155 (2008).
68. E. Bumrungthaichaichan, N. Jaiklom, A. Namkanisorn and S. Wattananusorn, *Sci. Res. Essays*, **11**(4), 42 (2016).
69. C. S. Mathpati, S. S. Deshpande and J. B. Joshi, *AIChE J.*, **55**(10), 2526 (2009).
70. L. S. Dautova, I. Milanovic and K. J. Hammad, in *2012 ASEE Northeast Section Conference*, University of Massachusetts Lowell (2012).
71. H. Rafiei, R. Janamiri, M. H. Sedaghat and A. Hatampour, *World Acad. Sci. Eng. Technol.*, **6**(12), 1189 (2012).
72. A. Parvareh, M. Rahimi and A. A. Alsairafi, *Iranian J. Chem. Eng.*, **6**(3), 3 (2009).
73. S. Y. Lee and B. W. Armstrong, *SDI CFD Modeling Analysis*, Savannah River National Laboratory, U.S.A. (2011).
74. S. Y. Lee, *Mixing Study for JT-71/72 Tanks*, Savannah River National Laboratory, U.S.A. (2013).
75. R. A. Leishear, S. Y. Lee, M. D. Fowley, M. R. Poirier and T. J. Steeper, *J. Fluids Eng.*, **134**, 111102-1 (2012).
76. I. R. Muhammad and J. P. Kizito, in *2012 ASME Early Career Technical Conference*, Georgia, U.S.A. (2012).
77. A. Egedy, B. Molnar, T. Varga and T. Chován, in *2014 COMSOL Conference*, Cambridge (2014).
78. M. Marek, T. Stoesser, P. J. W. Roberts, V. Weitbrecht and G. H. Jirka, in *32nd IAHR World Congress*, Venice, Italy (2007).
79. T. Stoesser, *Development and Validation of a CFD Code for Open-Channel Flows*, Ph.D. Dissertation, Department of Civil Engineering, Bristol University (2002).
80. O. Reynolds, *Philos. T. R. Soc. Lond.*, **186**, 123 (1895).
81. S. V. Patankar and D. B. Spalding, *Int. J. Heat Mass Tran.*, **15**, 1787

(1972).
82. ANSYS Inc., *ANSYS Fluent User's Guide: Release 15.0*, U.S.A. (2014).
83. ANSYS Inc., *ANSYS Fluent Theory Guide: Release 15.0*, U.S.A. (2013).
84. J. Zhu, *Commun. Appl. Numer. M.*, **7**, 225 (1991).
85. T. J. Barth and D. Jespersen, in *27th Aerospace Sciences Meeting*, Nevada, U.S.A. (1989).
86. E. M. Marshall and A. Bakker, in *Handbook of Industrial Mixing*, E. L. Paul, V. A. Atiemo-Obeng and S. M. Kresta Eds. John Wiley & Sons (2004).
87. R. Courant, K. Friedrichs and H. Lewy, *IBM J. Res. Dev.*, **11**(2), 215 (1967).
88. AIAA, *Guide for the Verification and Validation of Computational Fluid Dynamics Simulations*, American Institute of Aeronautics and Astronautics, U.S.A. (1998).
89. S. G. Gaikwad, *Studies in jet mixed tanks*, Master Thesis, University of Mumbai (2001).
90. G. N. Abramovich, *The Theory of Turbulent Jets*, MIT Press, Cambridge, MA (1963).
91. K. M. Kiser, *AIChE J.*, **9**(3), 386 (1963).
92. S. Post, *A Computational and Experimental Study of Near-Field Entrainment in Steady Gas Jets*, MSME Thesis, Purdue University (1998).
93. F. M. White, *Viscous fluid flow*, McGraw-Hill, New York (1974).
94. D. Shao and A. W. Law, *Environ. Fluid Mech.*, **10**, 521 (2010).
95. S. Ferrari, M. G. Badas, L. A. Besalduch and G. Querzoli, in *International Symposium on Turbulence and Shear Flow Phenomena*, France (2013).